Biochimica et Biophysica Acta 1853 (2015) 2033–2044

Contents lists available at ScienceDirect

Biochimica et Biophysica Acta

journal homepage: www.elsevier.com/locate/bbamcr

Annexin-A5 promotes membrane resealing in human trophoblasts☆

Romain Carmeille [a], Séverine A. Degrelle [b,c,d], Laurent Plawinski [a], Flora Bouvet [a], Céline Gounou [a], Danièle Evain-Brion [b,c,d], Alain R. Brisson [a], Anthony Bouter [a,*]

[a] Institute of Chemistry and Biology of Membranes and Nano-objects, UMR 5248, CNRS, University of Bordeaux, IPB, F-33600 Pessac, France
[b] Fondation PremUP, Paris, F-75006, France
[c] INSERM, U1139, Paris, F-75006, France
[d] Université Paris Descartes, UMR-S1139 Sorbonne Pris Cité, Paris, F-75006, France.

ARTICLE INFO

Article history:
Received 23 September 2014
Received in revised form 25 November 2014
Accepted 27 December 2014
Available online 14 January 2015

Keywords:
Membrane repair
Annexin-A5
Placenta
Trophoblast
Membrane resealing
Lesion removal

ABSTRACT

Annexin-A5 (AnxA5) is the smallest member of the annexins, a group of soluble proteins that bind to membranes containing negatively-charged phospholipids, principally phosphatidylserine, in a Ca^{2+}-dependent manner. AnxA5 presents unique properties of binding and self-assembling on membrane surfaces, forming highly ordered two-dimensional (2D) arrays. We showed previously that AnxA5 plays a central role in the machinery of cell membrane repair of murine perivascular cells, promoting the resealing of membrane damages via the formation of 2D protein arrays at membrane disrupted sites and preventing the extension of membrane ruptures. As the placenta is one of the richest source of AnxA5 in humans, we investigated whether AnxA5 was involved in membrane repair in this organ. We addressed this question at the level of human trophoblasts, either mononucleated cytotrophoblasts or multinucleated syncytiotrophoblasts, in choriocarcinoma cells and primary trophoblasts. Using established procedure of laser irradiation and fluorescence microscopy, we observed that both human cytotrophoblasts and syncytiotrophoblasts repair efficiently a μm^2-size disruption. Compared to wild-type cells, AnxA5-deficient trophoblasts exhibit severe defect of membrane repair. Through specifically binding to the disrupted site as early as a few seconds after membrane wounding, AnxA5 promotes membrane resealing of injured human trophoblasts. In addition, we observed that a large membrane area containing the disrupted site was released in the extracellular milieu. We propose mechanisms ensuring membrane resealing and subsequent lesion removal in human trophoblasts. This article is part of a Special Issue entitled: 13th European Symposium on Calcium.

1. Introduction

Plasma membrane disruption is a general phenomenon induced by mechanical stress in physiological conditions, which leads to the entry into cells of extracellular Ca^{2+} at mM concentration. Increase of intracellular Ca^{2+} concentration activates the repair protein machinery in eukaryotic cells ensuring a rapid resealing of large plasma membrane ruptures and preventing cell death [1–3]. Several models of membrane repair have been proposed, their occurrence probably depending on the size and the type of rupture [2,4]. The classical model of membrane repair is based on the formation of a lipid patch built by the fusion of intracellular vesicles, followed by the recruitment of this patch at the wounded site, which reseals the plasma membrane [5–8]. Recently it has been proposed that membrane repair relies primarily on exocytosis of lysosomal sphingomyelinase, which hydrolyses phosphorylcholine head group of sphingomyelin and induces the formation of ceramide-driven membrane invaginations, thus triggering lesion removal by an endocytic pathway [4,9]. Other groups have proposed that cell membrane repair occurs by removing membrane lesion through bleb formation [10] or shedding [11] using notably the ESCRT complex [12].

According to the classical model of membrane repair, mM-Ca^{2+} sensitive proteins, like dysferlin [13–15], MG-53 [16], AHNAK [17], calpains [18,19] and annexins [20–23], allow cytoplasmic vesicles to fuse and form a lipid patch, which is recruited to the damaged site of the plasma membrane. The membrane repair machinery starts to be identified, yet remains largely unknown. As defect in membrane repair is responsible for the development of muscular dystrophies such as limb–girdle muscular dystrophy type-2B and Miyoshi myopathy [13,14] and limb–girdle muscular dystrophy type-1C [24], major attention on membrane repair focused on skeletal muscle cells. Little is yet known on membrane repair in other tissues.

The human placental trophoblast is the primary barrier separating maternal blood from fetal blood. This epithelium-like tissue covering

Abbreviations: AnxA5, Annexin-A5; CT, cytotrophoblasts; D-PBS, Dulbelcco's phosphate buffer saline; PS, phosphatidylserine; ST, syncytiotrophoblasts

☆ This article is part of a Special Issue entitled: 13th European Symposium on Calcium.

* Corresponding author at: Bât. B14, Allée Geoffroy Saint Hilaire, 33600 Pessac, France. Tel.: +33 540006860; fax: +33 540002200.
E-mail address: a.bouter@cbmn.u-bordeaux.fr (A. Bouter).

http://dx.doi.org/10.1016/j.bbamcr.2014.12.038
0167-4889/

the placenta is a two-layered structure, the outer layer forming syncytia [25], named syncytiotrophoblasts (ST), which expands by fusion of underlying progenitor mononucleated cytotrophoblasts (CT) throughout pregnancy (Scheme 1). ST are the site of numerous placental functions including gas, ion and nutrient exchange and hormone synthesis required for fetal growth and development [26,27]. The trophoblastic layers protrude as finger-shaped villi in the intervillous space where the maternal blood circulates from the beginning of the second trimester. The apical membrane of ST is formed of very abundant but fragile microvilli bathing in maternal circulation. Surface expansion of the ST increases from 0.3-m^2 at 12 weeks of pregnancy to about 13-m^2 at term [25]. The number of CT fusing with preformed ST along pregnancy exceeds the required number for cell maintenance and growth [28]. The excess of material is shed from the syncytial surface into the maternal blood as ST-derived particles, named knots, sprouts or syncytial exosomes [29,30]. A very large amount of syncytial particles is shed per day, estimated at 4.7×10^4 and 8.5×10^5 particles for a 12-weeks and a 9-months placenta, respectively [25,31]. The molecular mechanisms leading to ST-derived particles shedding and the required processes of membrane repair at the site where a syncytial knot/sprout breaks away, are poorly understood. The revelation of the unexpected presence in ST of dysferlin, a major component of the muscle cell membrane repair machinery, hitherto supposed being specific to skeletal muscle, highlighted the existence of a machinery enabling an efficient plasma membrane repair in trophoblasts [32].

Disturbances of ST formation or functions are observed in pathological conditions. Preeclampsia, eclampsia and other pregnancy diseases are associated with exacerbated trophoblast deportation into maternal blood [33–37]. The deportation of trophoblast knots induces inflammatory response of maternal endothelial cells, directly involved in the physiopathology of preeclampsia [29]. As placental dysferlin expression drops by 38% in severe preeclampsia [38], a defect in membrane repair in preeclamptic ST may be hypothesized.

The annexins (Anx), a protein family presenting 12 members in humans, share the property of binding to negatively-charged lipid membranes, primarily those containing phosphatidylserine (PS) in a Ca^{2+}-dependent manner [39]. Several of their properties argue for their contribution in membrane repair processes such as their participation in numerous endo- and exo-cytic events by interaction with filamentous actin [40,41] and their ability to aggregate membranes [42,43]. During the last decade, many annexins have been shown to participate in membrane repair processes. AnxA1 and AnxA2 trigger intracellular vesicles fusion during the lipid patch formation and promote its attachment to the plasma membrane, by interacting with dysferlin at sarcolemma in normal muscle [20,21]. The absence of interactions between AnxA1-A2 and dysferlin is associated to a defect in membrane repair in dysferlinopathic mouse [20]. Recently, it has been shown that membrane repair of zebrafish skeletal muscle may be based on building of a highly ordered scaffold involving dysferlin, AnxA6, AnxA2 and AnxA1, in a chronological order [23]. Our group demonstrated that AnxA5 plays a critical role in membrane repair of murine perivascular cells by forming a two-dimensional (2D) array at the level of the torn membrane edges. This 2D array prevents wound expansion, which is due to the tension exerted by cytoskeleton, and promotes membrane resealing [22].

As the placenta is one of the richest source of AnxA5 in humans, we investigated whether AnxA5 was involved in membrane repair in this organ. First we assessed the ability of human trophoblasts to repair their plasma membrane and subsequently examined the role of endogenous and extracellular AnxA5 in this process. We addressed this question at the level of the human trophoblastic BeWo cell line and of human primary trophoblasts, either mononucleated CT or multinucleated ST. Using established procedures of laser irradiation and fluorescence microscopy, we compared the response of wild-type trophoblastic cells, which express constitutively AnxA5, and cells rendered deficient in AnxA5 by RNA interference. We found that endogenous AnxA5 promotes membrane resealing in both CT and ST, by interacting with plasma membrane at the injured site. The results achieved through this study led us to propose mechanisms for membrane resealing and lesion removal after membrane injury in human trophoblasts.

2. Materials and methods

2.1. Cell culture

Cell culture media and reagents were from Invitrogen (Thermo Fisher Scientific, Waltham, MA, USA) except when otherwise stated.

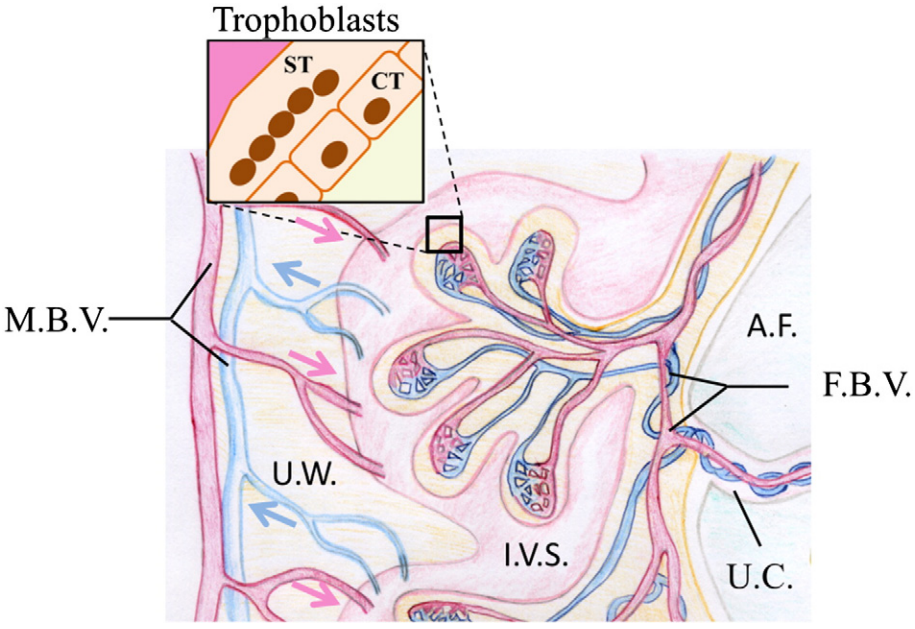

Scheme 1. Simplified scheme displaying trophoblasts localization in the placenta. A.F.: amniotic fluid; F.B.V.: fetal blood vessels; I.V.S.: intervillous space; M.B.V.: maternal blood vessels; U.C.: umbilical cord; U.W.: uterine wall.

All cell cultures were kept under standard conditions (37 °C, humidified atmosphere, 5% CO2).

2.1.1. Placental tissue collection and culture of primary trophoblasts

Term placentas were obtained after Caesarean section from healthy mothers with uncomplicated pregnancies delivered at 37–41 weeks of gestation. These biological samples were obtained following informed patient written consent and approval from local ethics committee (CCPPRB, Paris Cochin, N°18-05, Paris, France). Term villous CT were isolated from chorionic villi by differential sequential trypsin digestion and further purified on percoll gradient as previously described [44]. Cells were maintained in culture over 72 h in complete DMEM to form ST.

2.1.2. Culture of BeWo cells

The choriocarcinoma BeWo cell line was cultured in Ham's F12K medium supplemented with 20% fetal bovine serum, 5-mM L-glutamine, 100-units/mL penicillin and 100-μg/mL streptomycin and passaged twice a week to keep them in logarithmic growth. Differentiation and fusion of BeWo cells were induced by incubating the cells with 100-μM 8-Br-cAMP (Sigma) for 48-h in growth condition.

2.2. Western blotting

2.10^6 cells were trypsinized, pelleted and re-suspended in 300 μL of Dulbelcco's phosphate buffer saline (D-PBS) depleted in Ca^{2+} and supplemented with 1-mM EGTA. Protein extracts were obtained by sonicating the ice-cold cell solution with a Branson digital sonifier (amplitude 20%, duration 2-min, interval 5-s and pulse 5-s). Two successive centrifugations at 13,000-g for 1-min allowed to remove cell debris. 10-μg protein extracts were separated on a 10% SDS-PAGE. Semi-dry electrophoretic transfer (Bio-Rad) onto PVDF membrane was performed for 1-h at 100-V. The cellular content of AnxA5 and GAPDH (loading control) was detected with a mouse anti-AnxA5 monoclonal antibody (Sigma) and a rabbit anti-GAPDH polyclonal antibody (Santa Cruz), respectively. Both antibodies were diluted 1:1000 in saturation solution composed by Tris buffer saline (10-mM Tris, 150-mM NaCl, pH 8.0) supplemented with 0.1% Tween20 and 5% non-fat dry milk. Revelation was performed using secondary antibodies coupled to horse-radish peroxidase (Amersham) diluted 1:2000 in saturation solution and Opti-4CN™ colorimetric kit (Bio-Rad).

2.3. Membrane rupture and repair assay

BeWo cells and primary trophoblasts were cultured in complete growth medium without red phenol on 8-well Ibidi-treat μslide™ (Biovalley). Cells were incubated 5-min before acquisition with 5-μg/mL FM1−43FX (referred to hereafter as FM1−43 (Invitrogen)) in D-PBS and maintained over ice. To induce membrane damage, cells were irradiated at room temperature (20–21 °C), at 820-nm with a Chameleon-Vision™ mode-locked Titanium:Saphire laser (Coherent Inc, CA, USA) of a two-photon confocal scanning microscope (TCS SP2 AOBS, Leica) equipped with an HCX PL APO CS 63.0 × 1.40 oil-objective lens. Irradiation consisted of 3 successive scans (1.6 s per scan) of a 1-μm × 1-μm area with a power of 110-mW. 512 × 512 images were acquired at 1.6-s intervals with pinhole set to 1 Airy unit. For each condition, at least 100 cells from three independent experiments were analyzed. Two independent experiments are – conducted on different days, — performed on cells with different passage numbers and performed with freshly prepared FM1−43 and D-PBS solutions.

Membrane rupture and repair processes were monitored by measuring the variations in fluorescence intensity of FM1−43. FM1−43 was excited by the 488-nm laser line (intensity set at 40% of maximal power) and fluorescence emission was measured between 520-nm and 650-nm. For quantitative analysis, the fluorescence intensity was integrated over the whole cell surface and corrected for the fluorescence value recorded before irradiation, using ImageJ program. In order to characterize the magnitude and the rate of FM1−43 uptake, the fluorescence intensity changes were fitted according to the following "mono-exponential rise to maximum" equation [45]: Fluorescence Intensity = $(1 - \exp(-B * t)) * A$, where A corresponds to the maximal intracellular fluorescence intensity and B is equal to $Ln2/\tau_{½}$. This model implying the existence of a plateau, only repairing cells were therefore analyzed. Curve fitting was performed using Sigmaplot software (Systat Software inc., San Jose, USA).

2.4. Localization of endogenous AnxA5 in intact and damaged BeWo cells

For analysis in damaged BeWo cells, 2.10^5 cells were cultured in a 35-mm glass bottom dish equipped with a square-patterned coverslip (MatTek, Ashland, USA). Cell membrane rupture was performed according to the protocol described above, but in the absence of FM1−43 to avoid fluorescence cross-talk. Cells were fixed in 4% paraformaldehyde at room temperature after laser irradiation was completed. Fixation was terminated by adding 50-mM NH_4Cl. All subsequent steps (permeabilization, incubation with antibody and washes) were performed using 0.1% Triton X-100 and 1% BSA in D-PBS solution. Mouse anti-AnxA5 monoclonal antibody (Sigma) and secondary Alexa488-coupled anti-mouse goat antibody (Invitrogen) were successively incubated with cells for 1-h at 37 °C. Finally, cells were washed in D-PBS and a nuclear counterstaining was performed with DAPI (Sigma). For each condition, about 10 cells from three independent experiments were analyzed.

For analysis of intact cells, 2.10^4 cells/cm^2 were cultured in 8-well Ibidi-treat μslide™. Cells were immunostained employing the same protocol as described above for damaged cells from the step of paraformaldehyde fixation.

2.5. Localization of extracellular AnxA5 in damaged BeWo cells

Cells were incubated over ice in the presence of 3-μg.mL^{-1} Cy5-AnxA5 in D-PBS containing 1 mM Ca^{2+} for 5-min before irradiation. Cell membrane rupture was performed according to the protocol described above, but in the absence of FM1−43 to avoid fluorescence cross-talk. Cy5-AnxA5 was excited by the 633-nm laser line (intensity set at 60% maximal power) and its emission recorded between 650- and 750-nm.

2.6. Immunodetection of AnxA5 at the surface of undamaged trophoblastic cells

2.10^4/cm^2 primary trophoblasts or BeWo cells were cultured in 8-well Ibidi-treat μslide™. Live cells were incubated in the presence of anti-AnxA5 antibody coupled to Alexa488 for 45 min à 4 °C in D-PBS supplemented with 1-mM Ca^{2+}. After D-PBS washes, cells were fixed by 4% paraformaldehyde. As control, some cells were immunostained in the same conditions but after 4%-paraformaldehyde fixation and Triton X-100 permeabilization.

2.7. AnxA5-targetting siRNA transfection in BeWo CT

Reverse and forward siRNA transfection protocols were successively applied on 2.10^4 BeWo cells/cm^2. AnxA5-targetting siRNAs were from Invitrogen and consisted in a mix of two sequences: siRNA_A5_1 $^{5'}$GGGCUGAUGCAGAAACUCUUCGGAA$^{3'}$and siRNA_A5_2 $^{5'}$GAGGAAACCAUUGACCGCGAGACUU$^{3'}$. Transfection protocol (for 2.10^4 cells) consisted in incubating 2-pmol of AnxA5-targetting siRNAs and 0.6-μL RNAimax™ lipofectant solution (Invitrogen) in 50 μL Optimem, for 30-min at room temperature. The mixture was added drop-by-drop on trypsinized cell suspension (Reverse method) or adherent cells (Forward method) maintained in growth medium depleted in antibiotics. After 4-h incubation at 37 °C, transfection medium was replaced

by growth medium. Cells were analyzed 48 h after the forward transfection.

2.8. AnxA5-targetting shRNA lentiviral particle transduction in BeWo ST

The following shRNA sequences, cloned into the pLKO.1 puro-vector (MISSION® shRNA plasmids, Sigma), were used:

AnxA5-targetting shRNA: 5′-CCGGCGCGAGACTTCTGGCAATTTACTC GAGTAAATTGCCAGAAGTCTCGCGTTTTT-3′; Control non-target shRNA: 5′-CCTAAGGTTAAGTCGCCCTCGCTCGAGCGAGGGCGACTTA ACCTTAGG-3′.

Lentiviral-based particles containing shRNAs were produced by Bordeaux University Lentiviral Vectorology Platform (US005, Bordeaux, France) by transient transfection of 293 T cells. Bewo cells were plated at 2.10^4 cells per well in 8-well Ibidi-treat μslide™ and incubated for 24-h in complete medium. Transduction was carried out by adding concentrated lentiviral particles to the cells at multiplicity of infection of 30 in complete medium depleted in antibiotics for 24-h. The medium was then replaced with fresh complete medium supplemented with 100-μM 8-BrcAMP for 24-h. Cells were subsequently incubated with complete medium containing 1-μg/ml puromycin (Sigma) in order to select transduced cells. 24-h after antibiotic treatment, membrane repair assays were performed as described above.

3. Results

3.1. Membrane repair assay in human trophoblasts

In order to examine membrane repair ability of human trophoblasts at the level of CT and ST, BeWo cells were cultured either in the absence or in the presence of 100-μM 8-Br-cAMP for 48 h, respectively. Whereas BeWo cells remain as mononucleated cells (hereafter referred as BeWo CT) in free-cAMP growth condition, they differentiate and fuse in the presence of cAMP, forming large multinucleated cells (hereafter referred as BeWo ST). Typical images of BeWo CT and BeWo ST are presented in Figure S1.

We applied a well-established protocol of cell membrane disruption based on near infra-red laser irradiation [14,22]. By focusing the laser on plasma membrane for a few seconds, a μm^2-size membrane rupture was created in a controlled and highly reproducible way. To assess membrane disruption and repair, cells are irradiated in the presence of FM1–43, a water-soluble dye which becomes fluorescent upon inserting into lipid membranes, yet is unable to cross membranes. Therefore, cells with damaged plasma membrane exhibit an increase of fluorescence intensity due to the passive entrance of FM1–43 molecules into the cytosol and their incorporation into intracellular membranes. The process of membrane repair is monitored by time-lapse imaging of cytoplasmic FM1–43 fluorescence intensity after irradiation. Membrane resealing leads to a stop in the entry of FM1–43 molecules into the cytosol and therefore to a stop in the increase of the intracellular fluorescence intensity.

Membrane repair assay was first performed on BeWo CT in the presence of 1-mM Ca^{2+} (Fig. 1A). Irradiation conditions were adjusted (110-mW) to cause mild membrane injury to cells, as indicated by the absence of a large disruption at the irradiated site (Fig. 1A-frame 2, arrow). The cytoplasmic fluorescence intensity increased locally as early as a few seconds after irradiation (Fig. 1A-frames 2–3), indicating the presence of a membrane rupture. 120-s after plasma membrane disruption (Fig. 1A-frame 4), we observed that entry of FM1–43 remained limited to an area close to the disruption site. Analysis of the kinetics of intracellular fluorescence intensity variations showed that fluorescence increased for about 80-s and then reached a plateau (Fig. 1D, blue filled circles). The plateau indicated that entrance of FM1–43 molecules stopped and therefore that plasma membrane had resealed. Ca^{2+} is known to be a crucial component of membrane repair processes by activating most, if not all, of the steps of membrane resealing. As a control experiment, BeWo CT were irradiated in the absence of Ca^{2+} (Fig. 1B). In this condition, damaged BeWo CT exhibited a large entry of FM1–43 within the cell, characterized by a continuous and large increase of intracellular fluorescence intensity (Fig. 1D, blue filled triangles). This result indicated the absence of membrane resealing and validated the assay. When BeWo ST were submitted to the same irradiation conditions in the presence of 1-mM Ca^{2+}, these cells exhibited an increase of intracellular fluorescence limited to an area of a few μm^2 around the disruption site (Fig. 1C). The FM1–43 fluorescence intensity was observed to increase for a few seconds and then to reach a plateau (Fig. 1D, blue empty circles), indicating that cell membrane resealed rapidly. In the absence of Ca^{2+}, BeWo ST are unable to reseal their plasma membrane (Fig. S2), indicating that membrane resealing is also strictly Ca^{2+}-dependent in these cells. In order to characterize the membrane resealing process, the magnitude (A) and the rate ($\tau_{1/2}$) of FM1–43 uptake were determined (Fig. 1E). A and $\tau_{1/2}$ are respectively about eight and fifteen times lower for BeWo ST compared to BeWo CT. These two parameters indicate an enhanced ability of BeWo ST to reseal damaged plasma membrane.

The membrane repair assay was applied to human primary trophoblastic cells isolated from term placenta of healthy mothers. Primary CT differentiate and fuse spontaneously over three days of culture. Membrane repair ability of primary CT and ST were therefore investigated 24 h and 72 h after seeding, respectively. Primary trophoblasts behaved like BeWo cells, both of them are able to reseal their plasma membrane, with a more efficient repair for ST (Fig. 1D, black empty circles, and Fig. S3) compared to CT (Fig. 1D, black filled circles, and Fig. S3). We observed that the A and $\tau_{1/2}$ parameters are higher for primary cells compared to BeWo cells (Fig. 1E), indicating a faster process of resealing in BeWo cells. Many cell debris were observed in the medium during the assay (Fig. S3, arrowheads), suggesting a high fragility of primary cells. For this reason, we performed most of the further experiments with BeWo cells.

3.2. AnxA5 expression in human trophoblasts

By Western-blot analysis, we examined the relative expression of AnxA5 in BeWo cells and in human primary trophoblasts at the cyto- and syncytio-trophoblastic levels. AnxA5 is expressed at a similar level in BeWo CT and BeWo ST (Fig. 2A, left-hand lanes). The amount of endogenous AnxA5 was estimated at 3.5-ng/μg protein extract in both cell states. Primary CT and ST also expressed AnxA5 in a similar level with a concentration about three times higher than BeWo cells (Fig. 2A, middle lanes). We conclude therefore that AnxA5 is expressed at similar level in human CT and ST.

3.3. Subcellular distribution of endogenous AnxA5 in human trophoblasts

As we previously proposed that the formation of AnxA5 2D array at plasma membrane damaged sites was responsible for a strengthening of the membrane preventing the expansion of membrane tears [22], we investigated the subcellular localization of endogenous AnxA5 in intact and membrane-damaged BeWo cells. In intact cells, we observed that AnxA5 localizes in the nucleus and in the cytoplasm of BeWo CT (Fig. 2B, upper line) and BeWo ST (Fig. 2B, bottom line), in agreement with previous studies in BeWo cells [46] and other cell lines [47]. Primary CT and ST displayed the same subcellular localization of AnxA5 (Fig. S4). The homogenous distribution of AnxA5 within the cytoplasm supposes that it localizes in the cytosol. Some BeWo CT exhibited a stronger staining along the plasma membrane, exclusively localized at the cell–cell contacts (Fig. 2B, top left, arrowheads). This result correlates with a pleated shape of plasma membrane, as observed in DIC microscopy (Fig. 2B, top right, arrowheads). This stronger staining most

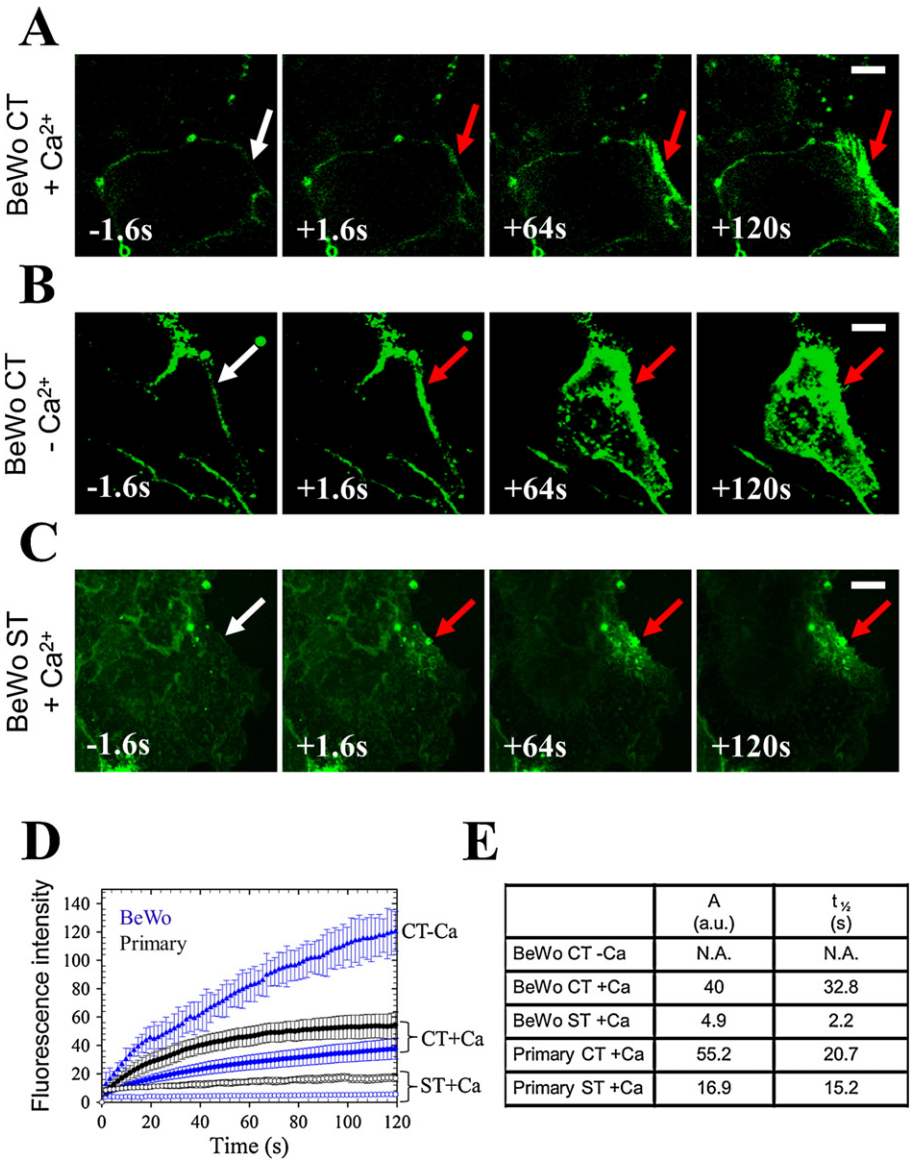

	A (a.u.)	$t_{½}$ (s)
BeWo CT -Ca	N.A.	N.A.
BeWo CT +Ca	40	32.8
BeWo ST +Ca	4.9	2.2
Primary CT +Ca	55.2	20.7
Primary ST +Ca	16.9	15.2

Fig. 1. Responses of human trophoblasts to membrane injury by laser irradiation. (A) Sequence of representative images showing the response of a BeWo CT to 110-mW infrared laser irradiation in the presence of 1 mM Ca^{2+}. (B) Sequence of representative images showing the response of a BeWo CT to 110-mW infared laser irradiation in the presence of 1 mM EGTA. Before irradiation, cells were washed 3 times in D-PBS devoid of Ca^{2+} and subsequently incubated in D-PBS supplemented with 1 mM EGTA for 5-min. (C) Sequence of representative images showing the response of a BeWo ST to 110-mW infrared laser irradiation in the presence of 1 mM Ca^{2+}. In all Figures, the area of membrane irradiation is marked with a white arrow before irradiation and a red arrow after irradiation. Image frames 1 and 2 were recorded 1.6 s before and 1.6 s after irradiation, respectively; Image frames 3–4 were recorded 64 s and 120 s after irradiation, respectively, as indicated. Scale bars = 20 μm. (D) Kinetic data represent the FM1−43 fluorescence intensity integrated over whole cell sections, averaged for 30 cells (+/− SD) and 100 cells (+/− SD) for primary and BeWo cells, respectively. In the presence of 1-mM Ca^{2+} (+Ca), the fluorescence intensities reach a plateau within the time of experiment for BeWo CT (blue filled circles), BeWo ST (blue empty circles), primary CT (black filled circles) and primary ST (black empty circles) indicating cell membrane reseals. In the absence of Ca^{2+} (−Ca), the fluorescence intensity measured in BeWo CT (blue filled triangles) increases continuously and is significantly larger than for the four other conditions. This result indicates the absence of membrane resealing. (E) Fluorescence intensity changes (mean values from (D)) were fitted according to the "mono-exponential rise to maximum" equation. A and $\tau_{1/2}$ refer respectively to the maximal fluorescence intensity and the time required to observe the half-maximum fluorescence intensity. N.A. and a.u. stand for "not applicable" and "arbitrary unit", respectively. A and $\tau_{1/2}$ are systematically lower for ST compared to CT, indicating an enhanced ability of ST to reseal damaged plasma membrane.

likely corresponds to a larger thickness at the contact region between two cells rather than a membrane localization.

We then assessed the subcellular localization of AnxA5 in laser-injured BeWo cells. Most previous studies dealing with the dynamics of intracellular proteins during cell membrane rupture and repair, have been based on the use of fluorescent fusion proteins [12,16,23]. Nevertheless, it remains elusive how an endogenous protein coupled to a 30-kDa fluorescent protein may fully conserve its traffic and protein interaction properties within the cell. Here we opted for studying resident endogenous AnxA5 using tools developed for correlative microscopy. BeWo cells were cultured in glass bottom dishes equipped with a square-patterned coverslip displaying an alphanumerical code in each square, thus enabling accurate tracking of irradiated cells. After irradiation, cells were fixed, permeabilized and immunostained for AnxA5. The localization of AnxA5 was studied for various time intervals (from 5 to 15-min) between irradiation and fixation. 5-min after laser injury, endogenous AnxA5 was found to accumulate specifically at the disruption site of BeWo CT and ST (Fig. 2C, upper frames). Strikingly, the presence of AnxA5 at the rupture site was retained in about 50% of cells fixed 15-min after plasma membrane disruption (Fig. 2C, bottom frames). When similar experiments were performed in buffer devoid of Ca^{2+}, we did not detect the presence of AnxA5 at the disrupted site, indicating its recruitment is strictly Ca^{2+}-dependent (data not shown). It has been reported that intracellular Ca^{2+} concentration drops rapidly to its initial

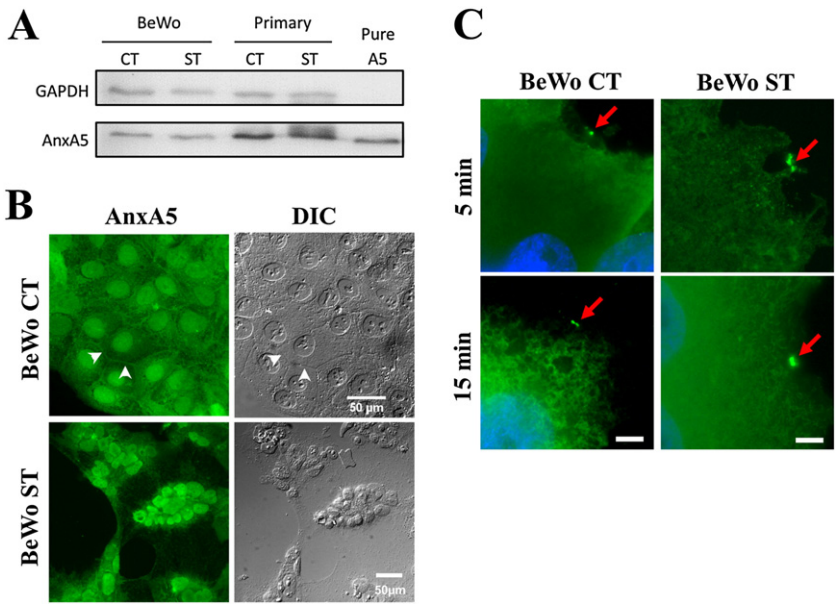

Fig. 2. Expression and subcellular distribution of endogenous AnxA5 in intact and damaged human trophoblasts. (A) The cellular content of AnxA5 in BeWo CT, BeWo ST, primary CT and primary ST was quantified through Western blot analysis, by comparison with 50-ng purified recombinant AnxA5 (Pure A5). 10-µg protein extract were separated on a 10% SDS-PAGE. AnxA5 and GAPDH (loading control) were respectively detected with a mouse anti-AnxA5 monoclonal antibody and a rabbit anti-GAPDH monoclonal antibody. The amount of endogenous AnxA5 was estimated at 3.5 ng/µg protein extract and 10 ng/µg protein extract in BeWo cells and primary trophoblasts, respectively. (B) Subcellular localization of endogenous AnxA5 in intact BeWo CT (upper line) and intact BeWo ST (bottom line) was analyzed by immunocytofluorescence. Cells were observed by fluorescence microscopy for AnxA5 (green) and by differential interference contrast microscopy (DIC). Scale bar = 50 µm. (C) Subcellular localization of endogenous AnxA5 in damaged BeWo CT (left-hand column) and damaged BeWo ST (right-hand column) was analyzed by immunocytofluorescence. Cells were irradiated with a 110-mW infrared laser in D-PBS containing 1-mM Ca^{2+} and fixed in 4% paraformaldehyde solution 5-min (upper panels) and 15-min (bottom panels) after laser irradiation was completed. Cells were immunostained for AnxA5 (green) and counterstained with DAPI (blue). The area of membrane irradiation is marked with a red arrow. Scale bar = 10 µm.

level (µM range) as early as a few seconds after membrane resealing [11,12]. Given that AnxA5 is known to be released from the membrane when Ca^{2+} concentration falls below 0.2-mM [48], its presence at damaged membrane site several minutes after resealing suggests that it is trapped in poorly accessible environments. The size of the fluorescent area where AnxA5 accumulated remained constant with time, estimated at 4 (±2)-µm^2 and 6 (±3)-µm^2 for BeWo CT and BeWo ST, respectively. As we did not observe interaction between AnxA5 and plasma membrane anywhere else in the irradiated cells, we conclude that resident endogenous AnxA5 binds exclusively to the disruption site of laser-injured plasma membrane.

When laser-injured BeWo CT and BeWo ST (data not shown) were immunostained for AnxA5 without the permeabilization step, we observed that a significant part of AnxA5 was accessible to antibodies at the level of disruption site (Fig. 3). The possibility that antibodies entered the cell due to the action of paraformaldehyde was ruled out by the absence of staining at other places than the disrupted site. We observed that the size of fluorescent areas formed by endogenous AnxA5 at disrupted sites in permeabilized (Fig. 2C) and non-permeabilized cells (Fig. 3, around 4-µm^2) were similar. This result indicates that, among the AnxA5 molecules accumulating at the disrupted site, a large part of them either interacts with the outer leaflet of the plasma membrane as soon as the disruption occurs or interacts with the inner leaflet when rupture is occurring and is excluded from the cytosol when membrane reseals.

3.4. Binding of extracellular AnxA5 to human intact and damaged trophoblasts

Some studies have reported the existence of AnxA5 in the extracellular milieu [49,50]. In the human placenta, it has been suggested that extracellular AnxA5 may cover the ST layer [51], preventing blood coagulation [52]. We investigated therefore whether AnxA5 molecules were constitutively associated with the outer leaflet of the plasma membrane in non-injured BeWo and primary CT and ST. Live cells were incubated

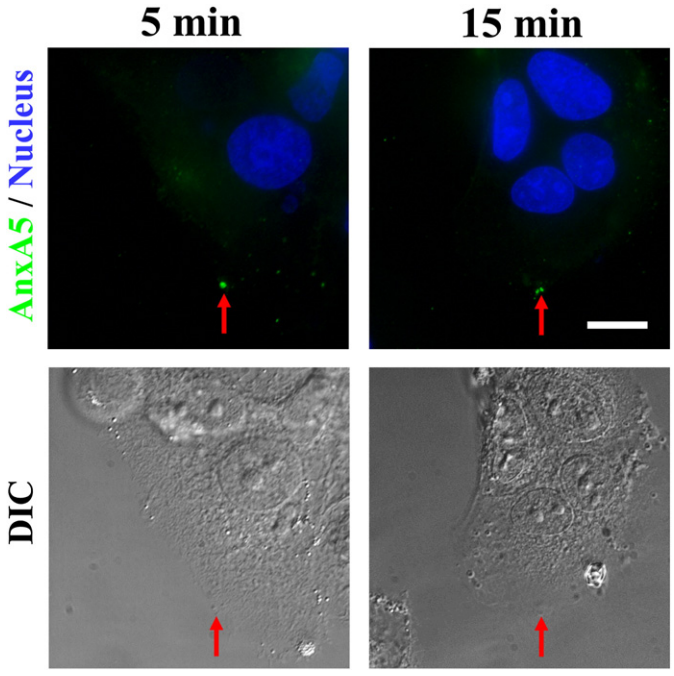

Fig. 3. Subcellular localization of endogenous AnxA5 in un-permeabilized laser-injured BeWo cells. Subcellular localization of endogenous AnxA5 in damaged BeWo CT was analyzed by immunocytofluorescence without the permeabilization step. Cells were irradiated with a 110-mW infrared laser in D-PBS containing 1-mM Ca^{2+} and fixed in 4% paraformaldehyde solution 5-min (left-hand column) and 15-min (right-hand column) after laser irradiation was completed. Cells were immunostained for AnxA5 (green) and counterstained with DAPI (blue). The area of membrane irradiation is marked with a red arrow. Scale bar = 20 µm.

45-min with fluorescent monoclonal antibody directed against AnxA5 in the presence of 1-mM Ca^{2+}. Incubation was performed at 4 °C in order to prevent, or slow down, endocytosis and to reduce unspecific entry of antibody into the cell. In these conditions, most BeWo CT showed no fluorescence at all (Fig. 4A). The only few BeWo CT that were labeled displayed an altered morphology, characteristic of an apoptotic or necrotic state (Fig. 4A, arrow). Control experiment confirmed the capacity of anti-AnxA5 antibody to interact with AnxA5 in these conditions of incubation (Fig. 4B). Similar results were found with primary CT (Fig. 4C) and ST (Fig. 4D), which allow us to conclude that AnxA5 is not constitutively present ex vivo at the surface of non-injured CT and ST.

In order to analyze the behavior of extracellular AnxA5 during cell membrane rupture, we irradiated BeWo cells in the presence of exogenously-added Cy5-AnxA5. Before membrane rupture, no AnxA5 staining was observed, indicating the absence of free PS exposed at the cell surface (Fig. 5, frame 1). As soon as 1.6-s after laser-injury of BeWo CT, extracellular AnxA5 was observed localizing exclusively at the disrupted site (Fig. 5, frame 2). Extracellular AnxA5 continued to accumulate at the disruption site for at least 1-min after laser irradiation (Fig. 5, frame 3–4). Similar results were obtained with BeWo ST (Fig. S5).

Since intact ST and CT do not expose PS at the cell surface, we conclude that binding of exogenous AnxA5 to membrane damaged areas in laser-irradiated cells reflects the transient and local exposure of PS molecules present in the inner leaflet of the plasma membrane.

We conclude also that both endogenous and exogenous AnxA5 molecules are able to be recruited at disruption site within 2- s after membrane injury.

3.5. Membrane repair ability of human AnxA5-deficient trophoblasts

In order to investigate the possible consequences of the absence of endogenous AnxA5 for membrane repair in trophoblastic cells, BeWo CT were transfected with AnxA5-targetting siRNAs. 48-h after two successive siRNA transfections, the content of endogenous AnxA5 in BeWo CT dropped by 90 ± 6% (n = 7), reaching a residual concentration of 0.3 (±0.08) ng/μg total protein extract (Fig. S6A). Immunocytochemistry analysis showed that transfected BeWo CT population was homogenously affected by AnxA5 knock-down (Fig. S6B).

When siRNA-transfected BeWo CT were submitted to cell membrane disruption, two types of response were observed. Most of transfected BeWo CT (67%) exhibited a large and deep entry of FM1–43 (Fig. 6A, upper panel), characterized by a strong and continuous increase of intracellular fluorescence intensity during the time of experiment (Fig. 6B, empty circles). This result indicates a defect of membrane resealing. The remaining 33% of cells behaved like un-transfected BeWo CT with an entry of FM1–43 limited to an area close to the plasma membrane (Fig. 6A, bottom panel), and a plateau of intracellular fluorescence intensity after about 100-s (Fig. 6B, filled circles); the repair kinetic parameters of these cells (Fig. 6C) were similar to those measured for un-transfected cells (Fig. 1E). The fact that about one third of cells within transfected cell population showed an efficient repair is likely to reflect the fact the transfection yield is not 100% and that some cells conserve a residual concentration of AnxA5 sufficient for achieving membrane resealing. We conclude therefore that the absence of endogenous AnxA5 leads to a defect of membrane repair in BeWo CT.

Several strategies were developed in order to establish AnxA5-deficient BeWo ST. We first tried to transfect BeWo CT with AnxA5-targetting siRNAs and subsequently to induce cell fusion by the addition of 8-BrcAMP. These cells were unable to fuse (data not shown). This observation indicates that AnxA5 may play a role in fusion of trophoblastic cells as it was proposed for myoblasts [53]. We also tried to transfect BeWo ST directly. However, the short lifetime of BeWo ST, together with their relative fragility, prevented us from obtaining a significant amount of viable cells. In addition BeWo ST surviving transfection steps exhibited a low decrease (inferior to 5%) of endogenous AnxA5 amount (data not shown). In order to overcome this problem, we decided to use shRNA lentiviral transduction strategy, which is particularly adapted for non-dividing cells. When BeWo ST were transduced with AnxA5-targetting shRNA lentiviral particles, we observed that most cells (75%) were unable to reseal laser-injured plasma membrane (Fig. 7A, upper panels and Fig. 7B, blue empty circles). Membrane repair was observed for the remaining 25% of cells (Fig. 7A, bottom panels and Fig. 7B, blue filled circles), which nevertheless exhibited a slower resealing characterized by kinetic parameters with A = 24.9 a.u. and $\tau_{1/2}$ = 11.5 s (Fig. 7C, A5-shRNA, 25%) instead of 9.8 a.u. and 10.2 s for BeWo ST transduced with lentiviral particles containing a scrambled shRNA sequence (Fig. 7B, black filled circles and Fig. 7C, ctrl).

We conclude that the absence of endogenous AnxA5 in human trophoblasts, at both CT and ST levels, leads to a defect in membrane repair.

3.6. Which mechanism ensures lesion removal in human trophoblasts?

During the course of this study we made the following observation that provides novel insight on the process of lesion removal. We observed with about half of BeWo and primary ST that the lipid material accumulated at the disrupted site was released from the cell after membrane resealing (Fig. 8). Two modus operandi were observed: either a

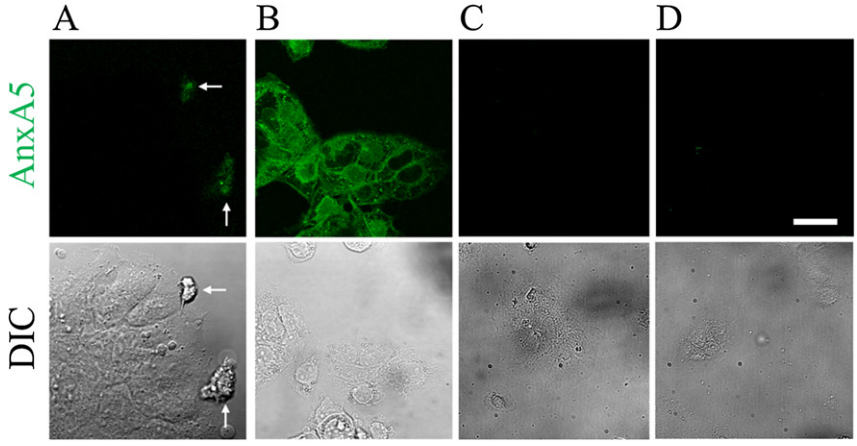

Fig. 4. Assessment of the presence of AnxA5 at the surface of human trophoblasts. Living BeWo CT (A and B) and primary CT (C) and ST (D) were incubated with monoclonal anti-AnxA5 antibody coupled to Alexa-488 for 45-min at 4 °C in the presence of Ca^{2+} (A, C and D). As control, a batch of BeWo CT was fixed, permeabilized and immunostained for AnxA5 in the same conditions (B). White arrows point out two cells and/or cell debris floating in the medium. No AnxA5 was detectable at the surface of human trophoblasts ex vivo (A, C and D). Scale bar = 40 μm.

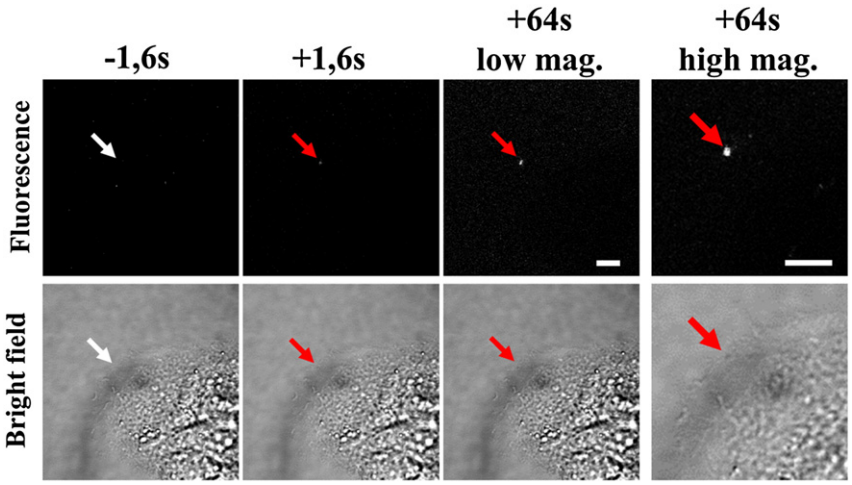

Fig. 5. Binding of extracellular AnxA5 to the disrupted site of injured membrane. Simultaneous recording in fluorescence microscopy (upper panels) and bright field microscopy (bottom panels) of a BeWo CT submitted to 110-mW laser-induced membrane rupture in the presence of 3-μg/ml Cy5-AnxA5 (white) diluted in D-PBS containing 1-mM Ca^{2+}. The area of membrane irradiation is marked with a white arrow before irradiation and a red arrow after irradiation. Image frames 1 and 2 were recorded 1.6 s before and 1.6 s after irradiation, respectively; Image frames 3 and 4 were recorded 64 s after irradiation. Image frame 4 is a high-magnified image from frame 3. Extracellular AnxA5 binds exclusively at the disrupted site of the injured membrane. Scale bars = 20 μm.

large fragment (about 100-μm^2) containing the wounding site moved away from the cell (Fig. 8A) or the area containing the disrupted site crumbled through membrane debris (about 5-μm^2) release (Fig. 8B and C). We observed that release of lipid material from the disrupted area began from 1-min or later after membrane disruption (Fig. 8, see also Fig. 1C), indicating that this process may correspond, not to

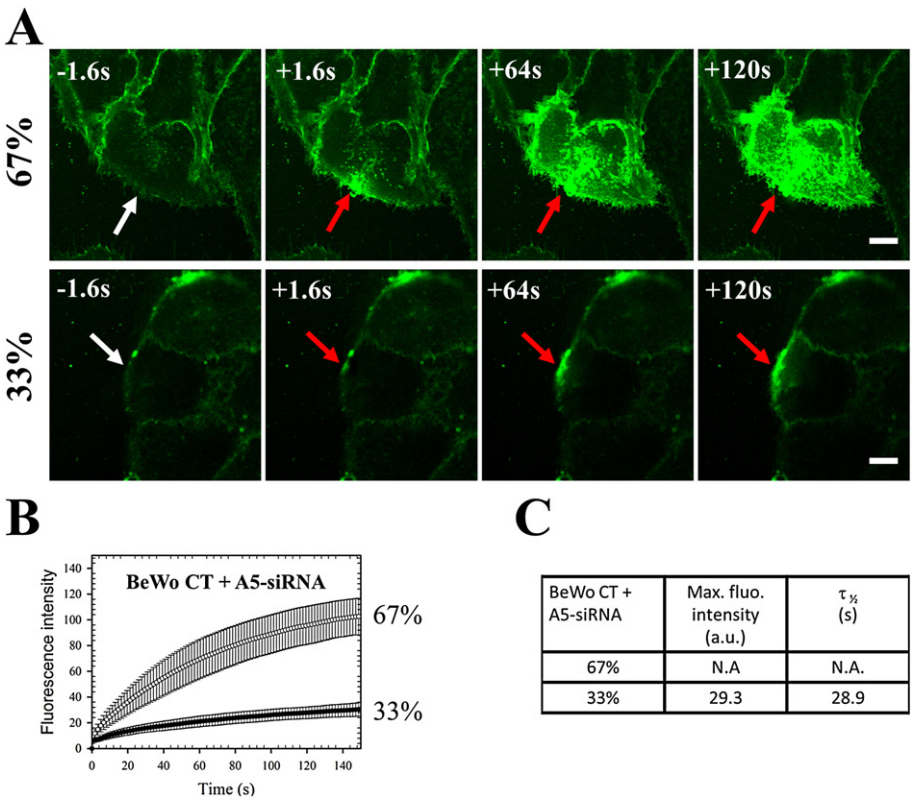

BeWo CT + A5-siRNA	Max. fluo. intensity (a.u.)	$\tau_{½}$ (s)
67%	N.A	N.A.
33%	29.3	28.9

Fig. 6. Responses of AnxA5-deficient BeWo CT to cell membrane injury. (A) Sequences of representative images showing the response of BeWo CT transfected with AnxA5-targetting siRNA to 110-mW infared-laser irradiation in the presence of 1-mM Ca^{2+}. Image series show two types of response: a minor fraction (about 33%, bottom panels) responds as observed for un-transfected cells with an entry of FM1–43 limited to a small area near the disruption site. A major fraction (about 67%, upper panels) presents a large increase of intracellular fluorescence intensity indicating the absence of membrane resealing. The area of membrane irradiation is marked with a white arrow before irradiation and a red arrow after irradiation. Image frames 1 and 2 were recorded 1.6 s before and 1.6 s after irradiation, respectively; Image frames 3–4 were recorded 64 s and 120 s after irradiation, respectively. Scale bars = 20 μm. (B) Kinetic data represent the FM1–43 fluorescence intensity integrated over whole cell sections, averaged for about 100 cells (+/− SD). For the minor fraction (33%, filled circles), the fluorescence intensity reaches a plateau within the time of experiment indicating cell membrane reseals. For the major fraction (67%, empty circles), the fluorescence intensity measured in AnxA5-targetting siRNA transfected BeWo CT increases continuously indicating the absence of membrane resealing. Fluorescence intensity changes (data from (B)) were fitted according to the "mono-exponential rise to maximum" equation. Mean values from membrane repair assays were used for this curve fitting. N.A. and a.u. stand for "not applicable" and "arbitrary unit", respectively.

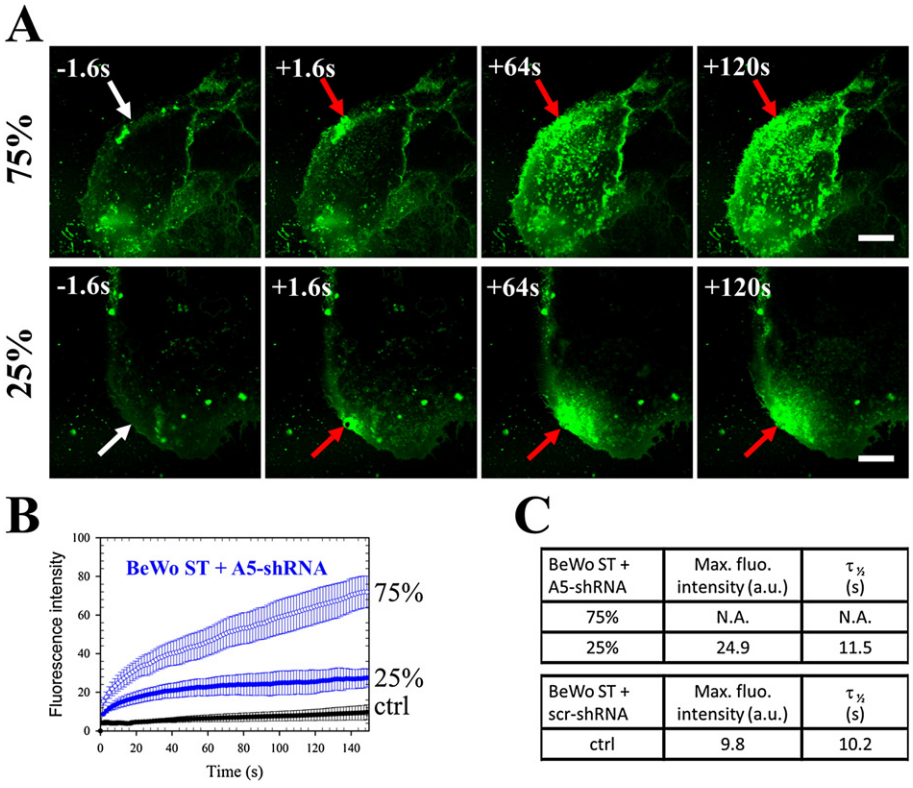

Fig. 7. Responses of AnxA5-deficient BeWo ST to cell membrane injury. (A) Sequences of representative images showing the response of BeWo ST transduced with lentiviral particles containing AnxA5-targetting shRNA to 110-mW infared-laser irradiation in the presence of 1-mM Ca^{2+}. Image series show two types of response: a minor fraction (about 25%, bottom panels) exhibits an increase of intracellular fluorescence, which stops within 1-min, indicating cell membrane reseals. A major fraction (about 75%, upper panels) presents a large increase of intracellular fluorescence intensity indicating the absence of membrane resealing. The area of membrane irradiation is marked with a white arrow before irradiation and a red arrow after irradiation. Image frames 1 and 2 were recorded 1.6 s before and 1.6 s after irradiation, respectively; Image frames 3–4 were recorded 64 s and 120 s after irradiation, respectively. Scale bars = 20 μm. (B) Kinetic data represent the FM1–43 fluorescence intensity integrated over whole cell sections, averaged for about 30 cells (+/− SD). For the minor fraction of BeWo ST transduced with AnxA5-shRNA (A5-shRNA) lentiviral particles (25%, blue filled circles), the fluorescence intensity reaches a plateau within the time of experiment indicating cell membrane reseals. For the major fraction (75%, blue empty circles), the fluorescence intensity increases continuously indicating the absence of membrane resealing. Kinetic data representing the response of BeWo ST transduced with lentiviral particles containing a scrambled shRNA are displayed (ctrl, black filled circles). (C) Fluorescence intensity changes (data from (B)) were fitted according to the "mono-exponential rise to maximum" equation. The parameters were calculated for kinetic data of BeWo ST transduced with AnxA5-shRNA (A5-shRNA, 25%) and scrambled shRNA (scr-shRNA, ctrl) lentiviral particles, which exhibited membrane resealing. Mean values from membrane repair assays were used for this curve fitting. N.A. and a.u. stand for "not applicable" and "arbitrary unit", respectively.

resealing mechanism, but to lesion removal. The 50% of remaining BeWo ST and all BeWo CT exhibited no beginning of wounded membrane release within the 2-min range of the membrane repair assay. Further investigations are required to determine what happens for these cells over a longer period.

4. Discussion

4.1. Human trophoblasts present an efficient repair machinery

The present study shows that ST reseal cell membrane disruption of μm^2-size within 30-s. This fast membrane resealing highlights the critical role of membrane repair processes for ST. Indeed, these syncytial cells, which form the outer layer of the trophoblastic tissue and protrude as finger-shaped villi in maternal blood, require protection and repair mechanisms in order to counteract the mechanical constraints induced by the shearing forces exerted by maternal circulation. Furthermore, ST are submitted to the continuous supply of cellular material provided by the fusion of underlying CT. Aging cytoplasmic content and nuclei are clustered and shed into the maternal circulation through ST-derived particles in 3–4 weeks [28,54]. It has been estimated that around 1×10^8 ST-derived particles are shed over the entire gestational period [25,29,31]. The molecular mechanism ensuring the formation of these particles and the required process of membrane repair after shedding, are poorly understood. A particular aspect to consider is that the various types of damages that may affect the ST plasma membrane will result in the exposure of PS-containing membranes to maternal blood. In view of the pro-coagulant properties of PS-exposing membranes, efficient mechanisms of membrane repair must operate in the placenta to prevent onset of blood coagulation, which could be life-threatening for the fetus.

The present study shows also that CT, although they are not in contact with maternal blood, reseal cell membrane disruption of μm^2-size within 100-s. The development and regeneration of ST require the fusion of underlying CT. By providing ST with a large part of their cellular content, CT may offer the main components of the repair machinery. It is noteworthy that dysferlin, a major membrane repair protein in skeletal muscle, may be lacking in CT [32]. This finding raises the essential issue of the role played by dysferlin in membrane repair in these cells. The possibility that the absence of dysferlin may be compensated by the presence of myoferlin [55] should be investigated.

4.2. AnxA5 promotes membrane resealing in human trophoblasts

Annexins have been shown to participate in membrane repair processes in numerous studies [20–23]. In this study, we focused our attention on AnxA5, because it is expressed at high level in the placenta, and because we reported previously its role in membrane resealing in murine perivascular cells [22]. CT and ST, rendered deficient in AnxA5 by RNA interference, suffer from a severe defect in membrane resealing, indicating that AnxA5 is a crucial component of the repair machinery in human trophoblasts. In a few seconds after membrane injury,

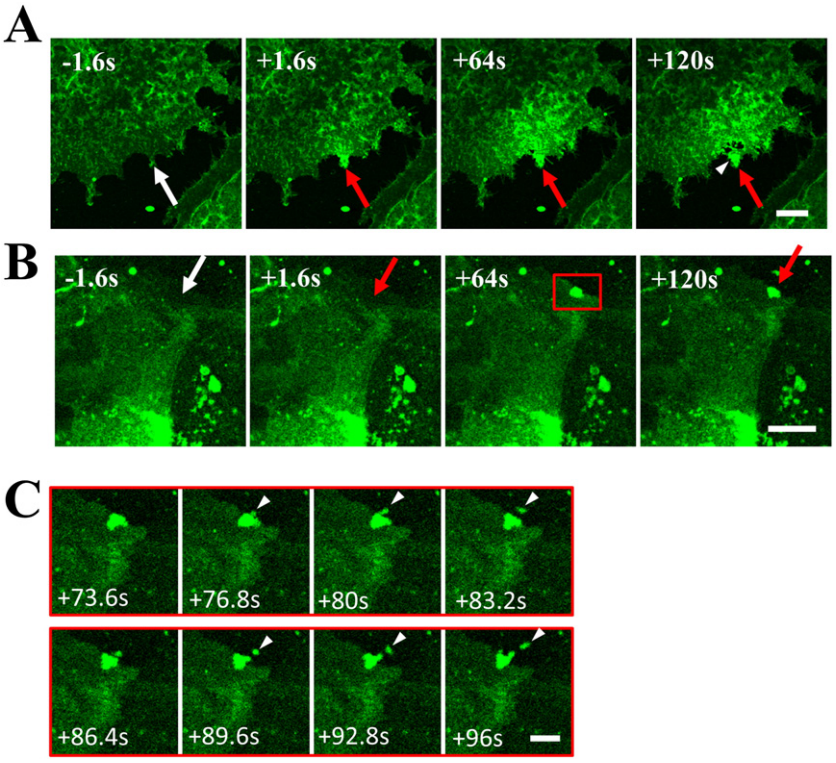

Fig. 8. Lesion removal of BeWo ST after cell membrane injury. (A) and (B) display two sequences of representative images showing two types of lesion removal from the disruption site of laser-injured BeWo ST. Cell membrane injury was performed through 110-mW infrared laser irradiation in the presence of 1 mM Ca^{2+}. In all figures, the area of membrane irradiation is marked with a white arrow before irradiation and a red arrow after irradiation. Image frames 1 and 2 were recorded 1.6 s before and 1.6 s after irradiation, respectively; Image frames 3–4 were recorded 64 s and 120 s after irradiation, respectively. In (A) the white arrowhead point out the removal of a large membrane fragment containing the disrupted site. In (B) the red square surrounds the area displayed in (C). Scale bar = 20 μm. (C) Two different time lapses showing the shedding of two successive membrane-derived debris (white arrowheads) from the disrupted site of the laser-injured BeWo ST displayed in (B). Scale bar = 10 μm.

endogenous AnxA5 is specifically recruited, in a Ca^{2+}-dependent manner, to the disruption site, where it is retained several minutes after membrane resealing. This result is consistent with the model we have proposed previously [22]. AnxA5, triggered by the local increase in Ca^{2+} entering the cell at mM-concentration, binds to PS molecules exposed at the edges of torn membranes, where it may self-assemble into 2D arrays. The formation of AnxA5 2D array may strengthen the membrane and prevent the expansion of the tear, by counteracting membrane tension due to the cortical cytoskeleton. The intracellular Ca^{2+} concentration has been found to drop rapidly after membrane resealing [11,12], at a level that is incompatible with AnxA5 binding to PS. The presence of AnxA5 several minutes after membrane resealing, suggests therefore it is trapped in a lipid environment where Ca^{2+} remains at mM concentration.

4.3. Which mechanisms ensure membrane resealing and lesion removal?

In wounded human trophoblasts, a large amount of lipid material accumulating at the disrupted site is detected as early as a few seconds after membrane disruption. Even if the nature of accumulating lipid material is not determined in our experiments, the variation of intracellular FM1–43 fluorescence intensity (see for instance Fig. 1C) suggests the cytoplasmic origin of this lipid material. Two main models of cell membrane repair are currently proposed. The classical model relies on Ca^{2+}-triggered fusion of intracellular vesicles, which may form a lipid patch enabling membrane resealing via an exocytosis-like process [5,7,8]. Besides, a new model has been recently proposed: Ca^{2+} entry through membrane disruption triggers exocytosis of lysosomes, which secrete acid sphingomyelinase in the extracellular milieu. Subsequently, hydrolysis of phosphorylcholine head group of sphingomyelin activates endocytosis, which mediates lesion removal [56,57]. It is unlikely that the fast membrane resealing observed in ST may be accomplished through ceramide-driven invagination induced by exocytosis of lysosomal enzymes. For instance, it was observed that secretion of significant amount of acid sphingomyelinase can take up to several minutes [57], inconsistent with a fast membrane resealing, in the second range. In addition, through specific binding to the disrupted site as early as a few seconds after membrane disruption, AnxA5 is a good reporter of the lesion fate. In most trophoblasts, AnxA5 is retained at the irradiated membrane region several minutes after membrane resealing. All together, these results prompt to propose that the formation of a lipid patch is likely responsible for membrane resealing in human trophoblasts.

Concerning the lesion removal in injured human trophoblasts, we frequently observed the shedding either of a large piece (about 100-μm^2) including the disrupted site or of burst of μm^2-size membrane debris from the lesion. This lesion removal begins at the earliest 1-min after membrane wounding. If released particles were already detected from SLO-perforated HEK293 cells [58], we report here, to our knowledge, the first direct evidence of the release of the plasma membrane wound.

5. Concluding remarks

Here we show that AnxA5 plays a central role in trophoblast membrane repair by promoting membrane resealing. We propose that the resealing process is primarily based on the formation of a lipid patch and that the lesion removal is managed through the release into the extracellular milieu of membrane material containing the wounded site. Whatever the membrane repair mechanism, we propose that AnxA5 achieves a universal and ubiquitous function, strengthening wounded plasma membrane through an early binding to the disrupted site after membrane injury. This binding prevents the extension of the tear by counteracting membrane tension due to the cortical cytoskeleton.

Several annexins have been shown to participate in plasma membrane repair [20–23,59], suggesting the annexin family forms an emergency team that orchestrates the cell membrane repair machinery, by protecting cells against the direct and collateral effects of plasma membrane rupture. Implication of other annexins, apart from AnxA5, in trophoblast membrane repair remains to be investigated. Furthermore, similarities and differences in mechanisms ensuring membrane repair in trophoblasts and other cell types remain elusive. Most studies dealing with membrane repair have focused until now on skeletal muscle, since it has been demonstrated that defect in membrane repair leads to muscular dystrophy [13,14,24]. Although a relationship between defective membrane repair and placental pathologies has not yet been clearly established, it is noteworthy that severe pre-eclampsia is associated with an expression of the trophoblastic dysferlin, a major component of the muscle repair machinery, dropped by 38% [38].

Acknowledgments

We thank Guillaume Pidoux and Pascale Gerbaud from Inserm S1139 UMR–Paris Descartes University for fruitful discussions. The fluorescence microscopy was done in the Bordeaux Imaging Center a service unit of the CNRS–INSERM and Bordeaux University, member of the national infrastructure France BioImaging. The help of Christel Poujol, Philippe Legros and Sébastien Marais is acknowledged. Lentiviral-based particles were produced by Bordeaux University lentiviral vectorology platform (US005, Bordeaux, France). The help of Alice Bibeyran, Véronique Guyonnet Dupérat and François Moreau-Gaudry is acknowledged. The project was supported by ANR (grant ANR-11-BSV1-0035 to A.R.B.) and by AFM-Téléthon (grant AFM-téléthon-17140 to A.B.).

Appendix A. Supplementary data

Supplementary data to this article can be found online at http://dx.doi.org/10.1016/j.bbamcr.2014.12.038.

References

[1] R.A. Steinhardt, G. Bi, J.M. Alderton, Cell membrane resealing by a vesicular mechanism similar to neurotransmitter release, Science 263 (1994) 390–393.
[2] P.L. McNeil, R.A. Steinhardt, Plasma membrane disruption: repair, prevention, adaptation, Annu. Rev. Cell Dev. Biol. 19 (2003) 697–731.
[3] P.L. McNeil, T. Kirchhausen, An emergency response team for membrane repair, Nat. Rev. Mol. Cell Biol. 6 (2005) 499–505.
[4] A. Draeger, E.B. Babiychuk, Ceramide in plasma membrane repair, Handb. Exp. Pharmacol. (2013) 341–353.
[5] K. Miyake, P.L. McNeil, Vesicle accumulation and exocytosis at sites of plasma membrane disruption, J. Cell Biol. 131 (1995) 1737–1745.
[6] M. Terasaki, K. Miyake, P.L. McNeil, Large plasma membrane disruptions are rapidly resealed by Ca^{2+}-dependent vesicle–vesicle fusion events, J. Cell Biol. 139 (1997) 63–74.
[7] P.L. McNeil, S.S. Vogel, K. Miyake, M. Terasaki, Patching plasma membrane disruptions with cytoplasmic membrane, J. Cell Sci. 113 (Pt 11) (2000) 1891–1902.
[8] G.Q. Bi, J.M. Alderton, R.A. Steinhardt, Calcium-regulated exocytosis is required for cell membrane resealing, J. Cell Biol. 131 (1995) 1747–1758.
[9] N.W. Andrews, P.E. Almeida, M. Corrotte, Damage control: cellular mechanisms of plasma membrane repair, Trends Cell Biol. 24 (2014) 734–742.
[10] E.B. Babiychuk, K. Monastyrskaya, S. Potez, A. Draeger, Blebbing confers resistance against cell lysis, Cell Death Differ. 18 (2011) 80–89.
[11] E.B. Babiychuk, K. Monastyrskaya, S. Potez, A. Draeger, Intracellular Ca(2+) operates a switch between repair and lysis of streptolysin O-perforated cells, Cell Death Differ. 16 (2009) 1126–1134.
[12] A.J. Jimenez, P. Maiuri, J. Lafaurie-Janvore, S. Divoux, M. Piel, F. Perez, ESCRT machinery is required for plasma membrane repair, Science 343 (2014) 1247136.
[13] J. Liu, M. Aoki, I. Illa, C. Wu, M. Fardeau, C. Angelini, C. Serrano, J.A. Urtizberea, F. Hentati, M.B. Hamida, S. Bohlega, E.J. Culper, A.A. Amato, K. Bossie, J. Oeltjen, K. Bejaoui, D. McKenna-Yasek, B.A. Hosler, E. Schurr, K. Arahata, et al., Dysferlin, a novel skeletal muscle gene, is mutated in Miyoshi myopathy and limb girdle muscular dystrophy, Nat. Genet. 20 (1998) 31–36.
[14] D. Bansal, K. Miyake, S.S. Vogel, S. Groh, C.-C. Chen, R. Williamson, P.L. McNeil, K.P. Campbell, Defective membrane repair in dysferlin-deficient muscular dystrophy, Nature 423 (2003) 168–172.
[15] L. Glover, R.H. Brown, Dysferlin in membrane trafficking and patch repair, Traffic 8 (2007) 785–794.
[16] C. Cai, H. Masumiya, N. Weisleder, N. Matsuda, M. Nishi, M. Hwang, J.-K. Ko, P. Lin, A. Thornton, X. Zhao, Z. Pan, S. Komazaki, M. Brotto, H. Takeshima, J. Ma, MG53 nucleates assembly of cell membrane repair machinery, Nat. Cell Biol. 11 (2009) 56–64.
[17] Y. Huang, S.H. Laval, A. van Remoortere, J. Baudier, C. Benaud, L.V.B. Anderson, V. Straub, A. Deelder, R.R. Frants, J.T. den Dunnen, K. Bushby, S.M. van der Maarel, AHNAK, a novel component of the dysferlin protein complex, redistributes to the cytoplasm with dysferlin during skeletal muscle regeneration, FASEB J. 21 (2007) 732–742.
[18] L.V. Anderson, R.M. Harrison, R. Pogue, E. Vafiadaki, C. Pollitt, K. Davison, J.A. Moss, S. Keers, A. Pyle, P.J. Shaw, I. Mahjneh, Z. Argov, C.R. Greenberg, K. Wrogemann, T. Bertorini, H.H. Goebel, J.S. Beckmann, R. Bashir, K.M. Bushby, Secondary reduction in calpain 3 expression in patients with limb girdle muscular dystrophy type 2B and Miyoshi myopathy (primary dysferlinopathies), Neuromuscul. Disord. 10 (2000) 553–559.
[19] T. Chrobáková, M. Hermanová, I. Kroupová, P. Vondrácek, T. Maríková, R. Mazanec, J. Zámecník, J. Stanek, M. Havlová, L. Fajkusová, Mutations in Czech LGMD2A patients revealed by analysis of calpain3 mRNA and their phenotypic outcome, Neuromuscul. Disord. 14 (2004) 659–665.
[20] N.J. Lennon, A. Kho, B.J. Bacskai, S.L. Perlmutter, B.T. Hyman, R.H. Brown, Dysferlin interacts with annexins A1 and A2 and mediates sarcolemmal wound-healing, J. Biol. Chem. 278 (2003) 50466–50473.
[21] A.K. McNeil, U. Rescher, V. Gerke, P.L. McNeil, Requirement for annexin A1 in plasma membrane repair, J. Biol. Chem. 281 (2006) 35202–35207.
[22] A. Bouter, C. Gounou, R. Bérat, S. Tan, B. Gallois, T. Granier, B.L. d' Estaintot, E. Pöschl, B. Brachvogel, A.R. Brisson, Annexin-A5 assembled into two-dimensional arrays promotes cell membrane repair, Nat. Commun. 2 (2011) 270.
[23] U. Roostalu, U. Strähle, In vivo imaging of molecular interactions at damaged sarcolemma, Dev. Cell 22 (2012) 515–529.
[24] C. Minetti, F. Sotgia, C. Bruno, P. Scartezzini, P. Broda, M. Bado, E. Masetti, M. Mazzocco, A. Egeo, M.A. Donati, D. Volonte, F. Galbiati, G. Cordone, F.D. Bricarelli, M.P. Lisanti, F. Zara, Mutations in the caveolin-3 gene cause autosomal dominant limb–girdle muscular dystrophy, Nat. Genet. 18 (1998) 365–368.
[25] K. Benirschke, P. Kaufmann, Pathology of the Human Placenta, Springer Science & Business Media, 2000.
[26] D. Evain-Brion, A. Malassine, Human placenta as an endocrine organ, Growth Hormon. IGF Res. 13 (Suppl. A) (2003) S34–37.
[27] W.W. Hay, Placental transport of nutrients to the fetus, Horm. Res. 42 (1994) 215–222.
[28] B. Huppertz, H.G. Frank, J.C. Kingdom, F. Reister, P. Kaufmann, Villous cytotrophoblast regulation of the syncytial apoptotic cascade in the human placenta, Histochem. Cell Biol. 110 (1998) 495–508.
[29] G.J. Burton, C.J.P. Jones, Syncytial knots, sprouts, apoptosis, and trophoblast deportation from the human placenta, Taiwan J. Obstet. Gynecol. 48 (2009) 28–37.
[30] C. Salomon, M.J. Torres, M. Kobayashi, K. Scholz-Romero, L. Sobrevia, A. Dobierzewska, S.E. Illanes, M.D. Mitchell, G.E. Rice, A gestational profile of placental exosomes in maternal plasma and their effects on endothelial cell migration, PLoS ONE 9 (2014) e98667.
[31] M.H. Abumaree, P.R. Stone, L.W. Chamley, An in vitro model of human placental trophoblast deportation/shedding, Mol. Hum. Reprod. 12 (2006) 687–694.
[32] D.D. Vandré, W.E. Ackerman, D.A. Kniss, A.K. Tewari, M. Mori, T. Takizawa, J.M. Robinson, Dysferlin is expressed in human placenta but does not associate with caveolin, Biol. Reprod. 77 (2007) 533–542.
[33] H. Alvarez, W.L. Benedetti, V.K. De Leonis, Syncytial proliferation in normal and toxemic pregnancies, Obstet. Gynecol. 29 (1967) 637–643.
[34] K. Benirschke, The human placenta J D Boyd and W J Hamilton Heffer, Cambridge, 365 pp 1970, Teratology 8 (1973) 77–78.
[35] M. Langbein, R. Strick, P.L. Strissel, N. Vogt, H. Parsch, M.W. Beckmann, R.L. Schild, Impaired cytotrophoblast cell–cell fusion is associated with reduced Syncytin and increased apoptosis in patients with placental dysfunction, Mol. Reprod. Dev. 75 (2008) 175–183.
[36] M. Johansen, C.W. Redman, T. Wilkins, I.L. Sargent, Trophoblast deportation in human pregnancy—its relevance for pre-eclampsia, Placenta 20 (1999) 531–539.
[37] M. Knight, C.W. Redman, E.A. Linton, I.L. Sargent, Shedding of syncytiotrophoblast microvilli into the maternal circulation in pre-eclamptic pregnancies, Br. J. Obstet. Gynaecol. 105 (1998) 632–640.
[38] C.T. Lang, K.B. Markham, N.J. Behrendt, A.A. Suarez, P. Samuels, D.D. Vandre, J.M. Robinson, W.E. Ackerman, Placental dysferlin expression is reduced in severe pre-eclampsia, Placenta 30 (2009) 711–718.
[39] V. Gerke, S.E. Moss, Annexins: from structure to function, Physiol. Rev. 82 (2002) 331–371.
[40] M.J. Hayes, U. Rescher, V. Gerke, S.E. Moss, Annexin–actin interactions, Traffic 5 (2004) 571–576.
[41] V. Gerke, C.E. Creutz, S.E. Moss, Annexins: linking Ca2+ signalling to membrane dynamics, Nat. Rev. Mol. Cell Biol. 6 (2005) 449–461.
[42] O. Lambert, V. Gerke, M.F. Bader, F. Porte, A. Brisson, Structural analysis of junctions formed between lipid membranes and several annexins by cryo-electron microscopy, J. Mol. Biol. 272 (1997) 42–55.
[43] D.S. Drust, C.E. Creutz, Aggregation of chromaffin granules by calpactin at micromolar levels of calcium, Nature 331 (1988) 88–91.
[44] J.L. Frendo, P. Thérond, T. Bird, N. Massin, F. Muller, J. Guibourdenche, D. Luton, M. Vidaud, W.B. Anderson, D. Evain-Brion, Overexpression of copper zinc superoxide dismutase impairs human trophoblast cell fusion and differentiation, Endocrinology 142 (2001) 3638–3648.
[45] G.W. Humphrey, E. Mekhedov, P.S. Blank, A. de Morree, G. Pekkurnaz, K. Nagaraju, J. Zimmerberg, GREG cells, a dysferlin-deficient myogenic mouse cell line, Exp. Cell Res. 318 (2012) 127–135.

[46] X. Wang, B. Campos, M.A. Kaetzel, J.R. Dedman, Secretion of annexin V from cultured cells requires a signal peptide, Placenta 22 (2001) 837–845.
[47] T. Skrahina, A. Piljić, C. Schultz, Heterogeneity and timing of translocation and membrane-mediated assembly of different annexins, Exp. Cell Res. 314 (2008) 1039–1047.
[48] R.P. Richter, J.L.K. Him, B. Tessier, C. Tessier, A.R. Brisson, On the kinetics of adsorption and two-dimensional self-assembly of annexin A5 on supported lipid bilayers, Biophys. J. 89 (2005) 3372–3385.
[49] M.J. Flaherty, S. West, R.L. Heimark, K. Fujikawa, J.F. Tait, Placental anticoagulant protein-I: measurement in extracellular fluids and cells of the hemostatic system, J. Lab. Clin. Med. 115 (1990) 174–181.
[50] J.F. Tait, M. Sakata, B.A. McMullen, C.H. Miao, T. Funakoshi, L.E. Hendrickson, K. Fujikawa, Placental anticoagulant proteins: isolation and comparative characterization four members of the lipocortin family, Biochemistry 27 (1988) 6268–6276.
[51] G. Krikun, C.J. Lockwood, X.X. Wu, X.D. Zhou, S. Guller, C. Calandri, A. Guha, Y. Nemerson, J.H. Rand, The expression of the placental anticoagulant protein, annexin V, by villous trophoblasts: immunolocalization and in vitro regulation, Placenta 15 (1994) 601–612.
[52] J.H. Rand, X.-X. Wu, Antibody-mediated interference with annexins in the antiphospholipid syndrome, Thromb. Res. 114 (2004) 383–389.
[53] E. Leikina, K. Melikov, S. Sanyal, S.K. Verma, B. Eun, C. Gebert, K. Pfeifer, V.A. Lizunov, M.M. Kozlov, L.V. Chernomordik, Extracellular annexins and dynamin are important for sequential steps in myoblast fusion, J. Cell Biol. 200 (2013) 109–123.
[54] T.M. Mayhew, Villous trophoblast of human placenta: a coherent view of its turnover, repair and contributions to villous development and maturation, Histol. Histopathol. 16 (2001) 1213–1224.
[55] J.M. Robinson, W.E. Ackerman, N.J. Behrendt, D.D. Vandre, While dysferlin and myoferlin are coexpressed in the human placenta, only dysferlin expression is responsive to trophoblast fusion in model systems, Biol. Reprod. 81 (2009) 33–39.
[56] V. Idone, C. Tam, J.W. Goss, D. Toomre, M. Pypaert, N.W. Andrews, Repair of injured plasma membrane by rapid Ca^{2+}-dependent endocytosis, J. Cell Biol. 180 (2008) 905–914.
[57] C. Tam, V. Idone, C. Devlin, M.C. Fernandes, A. Flannery, X. He, E. Schuchman, I. Tabas, N.W. Andrews, Exocytosis of acid sphingomyelinase by wounded cells promotes endocytosis and plasma membrane repair, J. Cell Biol. 189 (2010) 1027–1038.
[58] S. Potez, M. Luginbühl, K. Monastyrskaya, A. Hostettler, A. Draeger, E.B. Babiychuk, Tailored protection against plasmalemmal injury by annexins with different Ca2+ sensitivities, J. Biol. Chem. 286 (2011) 17982–17991.
[59] A. Draeger, K. Monastyrskaya, E.B. Babiychuk, Plasma membrane repair and cellular damage control: the annexin survival kit, Biochem. Pharmacol. 81 (2011) 703–712.